2016 24th International Lightning Detection Conference &
6th International Lightning Meteorology Conference
18 - 21 April | San Diego, California, USA

An Investigation of Radar-Derived Precursors to Lightning Initiation

Evan Ruzanski
Weather Research and Technology–Applied Meteorology
Vaisala, Inc.
Louisville, CO, USA
evan.ruzanski@vaisala.com

V. Chandrasekar
Dept. of Electrical and Computer Engineering
1373 Campus Delivery
Colorado State University
Fort Collins, CO, USA

***Abstract*—This study investigates the concept of predictability of lightning activity and related radar-based products. Analyses of predictability are done using a grid-based approach, where the concept of predictability is represented by de-cross-correlation time, or the automated forecasting (nowcasting) lead time where the cross correlation between the nowcasted quantity and the concurrent lightning flash rate density observations falls to a value of 1/*e*. Four storm events occurring over the Dallas-Fort Worth region were used for analysis. The results show that a vertically integrated radar reflectivity quantity estimating mixed-phase ice mass yielded predictability of about 14 min. The predictability of radar reflectivity values greater than 30 dB*Z* at an altitude corresponding to –10ºC was shown to about 10 min. Both of these radar-based quantities have previously been shown to be reliable precursors to lightning initiation. The predictability of the gridded lightning density fields was shown to be about 9 min.**

Keywords—Meteorological radar; Lightning; Ice; Prediction methods; Weather forecasting

I. INTRODUCTION

Accurate, spatially specific, and temporally extended short-term automated forecasts (nowcasts) of lightning activity are of great interest to the preservation of life and resources for a multitude of applications, such as aviation, defense, and large-venue operations. The measurement range and resolution of weather radar is favorable for effective nowcasting and weather radar data processing algorithms can estimate ice and graupel aloft, key components in the atmospheric electrification process.

The usefulness of using isothermal reflectivity (e.g., 30–40 dBZ at the –10ºC environmental height) for lightning nowcasting is supported by many studies [Dye et al., 1989; Buechler and Goodman, 1990; Gremillion and Orville, 1999; Vincent et al., 2003; Wolf, 2006; Yang and King, 2010;. Woodard et al., 2012] presented a comprehensive review and study of recent methods involving nowcasting radar products in the context of lightning activity. This study found that radar observations within the Larsen area (i.e., areas of reflectivity greater than 30 dBZ at an environmental height corresponding to −10° C) yielded the best results in terms of skill and lead time.

Carey and Rutledge [2000] modeled radar-estimated ice mass aloft using a simplified bulk microphysical model. Mosier et al. [2011] performed a comprehensive study of lightning nowcasting using a modified version of the Carey and Rutledge [2000] model that they called Vertically Integrated Ice (VII). Mosier et al. [2011] considered observations of VII trends in convective storm cells between two consecutive radar scans for many storms over Houston, TX, over a 10-year period. They found maximum lead times to lightning initiation to be about 19 and 14 min for isothermal reflectivity (i.e., 30 dBZ at the –10ºC environmental height) and VII, respectively. This and related later work by Seroka et al. [2012] used a cell-based approach for nowcasting and analysis, where storm cells were first identified before nowcasting and lightning activity was associated with that particular cell.

This paper presents a study to provide insight into the best manner and extent to nowcast lightning activity to a desired location using a grid-based analysis. This study extends previous work by analyzing the correlation structure between nowcasts of radar and lightning quantities in Lagrangian space using a grid-based approach. Whereas previous work identified and tracked radar features and observed a lead time to lightning activity associated with a particular cell, this analysis specifies a lead time and references that lead time to a point on the grid which represents the desired location at which a lightning forecast is made. Previous related studies have investigated the predictability of precipitation using nowcasts of radar reflectivity in a similar manner [Ruzanski and Chandrasekar, 2012]. Given that radar reflectivity is related as well to lightning flash rate density, such a similar approach is used in this work.

II. DATA AND DATA MODELS

A. Radar Data Model

The quantity known as Vertically Integrated Ice (VII), is given by Mosier et al. [2011] and is written as,

This work was supported by the National Science Foundation and Vaisala.

$$\mathrm{VII}(x,y) = 1000\pi\rho_i N_0^{\frac{3}{7}}\left(\frac{5.28\times10^{-18}}{720}\right)^{\frac{4}{7}}\times \int_{H_{-10}}^{H_{-40}} Z_H(x,y,H)^{4/7}dH, \quad (1)$$

where ρ_i is the density of ice, N_0 is the intercept parameter of an exponential size distribution of precipitation-sized ice, and H_{-10} and H_{-40} represent the heights of the –10°C and –40°C environmental levels, respectively. Equation (1) represents a measure of mixed-phase ice mass, a quantity Carey and Rutledge [2000] found to be strongly correlated with total lightning flash rate.

Mosier et al. [2011] followed previous work where ρ_i and N_0 are treated as variables with constant values 0.917 kg cm^{-3} and 4×10^6 m^{-4}, respectively. These parameters values were determined from a study Peterson [1997] performed in the Tiwi Islands region. Despite Carey and Rutledge [2000] stating the shortcomings and cautions of assuming constant values for these parameters, and noting significant intra-storm variability, following studies [Mosier et al., 2011; Seroka et al., 2012] have continued to make these assumptions. They claimed that making these assumptions was unrealistic but still acceptable for their studies that examined the relationship between lightning activity and trends of VII. Yet, Vamoş and Crăciun [2012] showed that that significant errors in VII values may lead to significant errors in the trends as well.

This study uses the hydrometeor classification algorithm described by Lim et al. [2005] to estimate the locations of ice from the radar reflectivity data. This algorithm identifies the following ice categories using dual-polarization variables: wet ice, low-density ice, high-density ice, hail, and rain–hail mix. Once identified, results from bulk microphysics studies are used to diagnose the parameters ρ_i and N_0 in the model described by (1). El-Magd et al. [2000] quantitatively compared multiparameter radar observations collected by the CSU-CHILL radar and *in situ* observations collected by a high-volume particle sampler probe mounted on a T-28 aircraft to yield density estimates of 0.55 kg cm^{-3} and 0.93 kg cm^{-3} for graupel and wet hail, respectively. Milbrandt and Yau [2005] considered bulk densities of 0.40, 0.50, and 0.90 kg cm^{-3} for moderate-density ice, high-density ice, and hail, respectively. Wainwright et al. [2014] developed power-law relationships between the intercept parameter of the exponential particle size distribution and the water content for the rain, hail, graupel, and snow hydrometeor categories within the Milbrandt and Yau microphysics scheme. They computed mean values of the intercept parameters for rain, snow, graupel, and hail from simulations of the Milbrandt and Yau scheme to be 1.18×10^5 m^{-4}, 3.95×10^8 m^{-4}, 5.26×10^7 m^{-4}, and 3.50×10^5 m^{-4}, respectively. The parameters used in the model described by (1) in this study are summarized in Table I.

B. Radar Data

The radar data used for this study were collected by the Weather Service Radar-1988 Doppler (WSR-88D) radar located near Fort Worth, TX (ICAO location identifier KFWS). The data were collected during four severe storm events occurring in April and May of 2014.

TABLE I. RADAR DATA MODEL PARAMETERS

Hydrometeor Classification	Radar Data Model Parameter Values	
	ρ_i (kg cm^{-3})	N_0 (m^{-4})
Wet ice	0.50	2.63×10^{7} [a]
Low-density ice	0.40	5.26×10^7
High-density ice	0.55	5.26×10^7
Hail	0.90	3.50×10^5
Rain-Hail mix	0.93	2.34×10^{5} [b]

[a] This is the mean value of the intercept parameters for rain and graupel found in the work by Wainwright et al. [2014].
[b] This is the mean value of the intercept parameters for rain and hail found in the work by Wainwright et al. [2014].

TABLE II. EVENT AND RADAR DATA MODEL PARAMETER DETAILS

Start Date (YYYYMMDD)	Details			
	Start time (UTC)	*End time (UTC)*	H_{-10} *(km)*	H_{-40} *(km)*
20140403	000335	235741	5.0	9.5
20140427	100458	160443	5.5	9.5
20140512	101356	235808	6.0	10.0
20140525	180517	040252	6.0	10.0

The data were processed into Constant Altitude Plan Position Indicator (CAPPI) frames with north–south and east–west grid spacing of 1 km covering an area within +/-100 km of the radar site at altitudes from 500 m to 12 km in 500-m increments. The approximate temporal resolution of the data is 4.5 min. Reflectivity values greater than 30 dBZ from the appropriate CAPPI (determined to be approximately the –10°C level from the soundings nearest Fort Worth at 0000 UTC on the respective event start date) and VII values computed according to (1) were used for analyses. Details of the data set used for evaluation are given in Table II.

C. Lightning Data

The lightning data used for this study were collected by processing detections of lightning discharges from multiple Vaisala LS-7002 VHF remote lightning sensors [Cummins and Murphy 2009] part of the National Lightning Detection Network (NLDN) [Orville, 2008] within approximately 1000 km of the KFWS WSR-88D radar. Distinguished intra-cloud and cloud-to-ground flash data were grouped together and were converted to flash density. The flash density data were processed to grids with 1 km north–south and east–west spacing at ground level covering an area of +/-100 km from the KFWS radar site. The total lightning data (i.e., aggregated cloud-to-ground and could-to-cloud) were considered for analyses.

D. Nowcasting Model

The Lagrangian persistence paradigm for nowcasting was used for this study. The Dynamic Adaptive Radar Tracking of Storms (DARTS) algorithm was used to generate the estimates of motion of radar and lightning quantities in this study [Ruzanski et al., 2011]. The DARTS model is built upon a modified general continuity equation, and can be represented as a discrete linear model, given by,

$$k_t F(k_x, k_y, k_t) =$$

$$-\left[\frac{1}{N_x N_y}\right]\sum_{k'_x=N_x^-}^{N_x^+}\sum_{k'_y=N_y^-}^{N_y^+}\left[\frac{U(k'_x,k'_y)}{T_x/T_y}\right](k_x-k'_x)F(k_x-k'_x,k_y-k'_y,k_t)-\left[\frac{1}{N_x N_y}\right]\sum_{k'_x=N_x^-}^{N_x^+}\sum_{k'_y=N_y^-}^{N_y^+}\left[\frac{V(k'_x,k'_y)}{T_x/T_y}\right](k_x-k'_x)F(k_x-k'_x,k_y-k'_y,k_t)-\left(\frac{i}{2\pi}\right)[T_t S(k_x,k_y,k_t)], \quad (2)$$

where $F(k_x, k_y, k_t)$ represents the 3-D DFT coefficients of the observed discrete radar field sequence, $U(k_x, k_y)$ represents the 2-D DFT coefficients of the field of estimated east-west motion vector components, $V(k_x, k_y)$ represents the 2-D DFT coefficients of the field of estimated north-south motion vector components, and $S(k_x, k_y, k_t)$ represents the 3-D DFT coefficients of the sequence of estimated evolution fields $S(n_x, n_y, n_t)$. T_x and T_y are the lengths of the horizontal and vertical dimensions of the observed gridded reflectivity fields, respectively, T_t is the number of reflectivity fields considered for motion estimation (i.e., the temporal span of the sequence of gridded reflectivity fields), and N_x and N_y are the maximum harmonic numbers of $F(k_x, k_y, k_t)$ in the horizontal and vertical dimensions, respectively.

Nowcasted fields are then generated by recursively advecting the latest observation or nowcast according to the (temporally fixed or persistent during the lead time period) motion vector fields estimated by DARTS via a backward mapping approach similar to the semi-Lagrangian backward scheme described by the work of Germann and Zawadzki [2002].

III. Experimental Procedure and Results

Nowcasts of radar reflectivity, VII, and lightning density were made out to 40 min using DARTS and the backward advection technique, where similar tuning of DARTS model parameters was used for each dataset. Example observations and corresponding 15-min nowcasts and estimated motion vector fields from the Apr 3, 2014, event are shown in Fig. 1. This figure provides example illustrations of each data product observation and nowcast, highlighting the differences of these as well as differences in the estimated motion vector fields. Note that because estimating the motion vector using model described by (2) involves Fourier transforms, motion vectors will be estimated in regions where no reflectivity was observed.

The cross-correlation coefficient used in this study is the estimate of the 2-D Pearson correlation coefficient, *r*, described by [Pearson, 1896],

$$r = \frac{\sum_m \sum_n (A_{mn}-\bar{A})(B_{mn}-\bar{B})}{\sqrt{(\sum_m \sum_n (A_{mn}-\bar{A})^2)(\sum_m \sum_n (B_{mn}-\bar{B})^2)}}, \quad (3)$$

where *A* is the nowcasted field, *B* is the time-aligned field of lightning flash rate density observations, and the overbar represents the sample mean.

Cross-correlation coefficients between each frame of the nowcast sequences and corresponding lightning density observations were computed. These results are shown in Fig. 2. The predictability is quantified by the *de-cross-correlation time*, which is defined as the lead time where the cross-correlation between the nowcasted quantity and the lightning observations decays to a value of 1/*e* (approximately 0.3679). This is considered to be the maximum lead time where the nowcasted quantities provide value, an approach used by previous related studies which investigated the predictability of precipitation patterns represented by radar observations [Ruzanski and Chandrasekar, 2012].

The results show that average de-cross-correlation times for the VII, isothermal reflectivity, and lightning are approximately 14, 10, and 9 min, respectively. These lead times are consistent with the results of previous studies [Mosier et al., 2011]. As expected, the lightning density field nowcasts exhibit highest cross-correlation with the lightning density observations for shorter lead times, seen here to be about 5–6 min. The utility of nowcasting the two radar products is exhibited for longer lead times. The extended predictability of VII can be attributed to the favorable initial cross-correlation with the lightning density fields and the favorable spatiotemporal coherence afforded by the vertical integration of radar reflectivity in the computation of VII described by (1). The relatively short de-correlation time for the lightning density fields suggests less spatiotemporal coherence innate to the lightning density fields relative to the radar fields.

IV. Summary and Conclusions

This paper presented a study to give insight into the best data product to use to nowcast lightning activity to a given location. The extent to which these data products can be nowcasted was investigated via cross-correlation analysis in Lagrangian space. The concept of de-cross-correlation time, or the maximum nowcasting lead time where the cross-correlation between the nowcast and corresponding lightning density observation decays to the point where it is no longer potentially valuable as a predictor of lightning activity, was introduced and investigated. This extends the cross-correlation and grid-based approach used in previous research investigating the predictability of precipitation patterns represented by radar reflectivity to radar–lightning relationships in Lagrangian space; whereas previous studies investigating lead time to lightning activity afforded by radar-based products tracked individual storm cells and determined lead time observationally, this study uses a grid-based areal approach with specified lead times for the analyses.

The results of the analysis of four severe storm events occurring over the Dallas-Fort Worth, TX, region over four events showed that a radar-based estimate of mixed-phase ice mass called the Vertically Integrated Ice, effectively a scaled vertical integration of radar reflectivity over altitudes related to lightning activity, yielded the longest average predictability (de-cross-correlation time) of about 14 min. The predictability of radar reflectivity values greater than 30 dB*Z* at an altitude corresponding to –10°C was shown to about 10 min. The predictability of both of these radar-based quantities were shown to be longer than that of the lightning density fields themselves. These lead times fall within the ranges of previous studies utilizing the cell-based analysis approach.

These results show the potential and provide a first-order approximation of an extent of using nowcasts of these radar-based quantities to nowcast lightning activity. Future work should include investigating a larger sample size of events at

more and various geographical locations and investigating performance in an operational sense using skill scores.

ACKNOWLEDGMENT

The authors would like to thank Mattia Vaccarono and Karthik Ganesan for their assistance with processing the hydrometeor classification data used in this study.

REFERENCES

Buechler, D. E., and S. J. Goodman (1990), Echo size and asymmetry: Impact on NEXRAD storm identification, J. Appl. Meteor., 29, 962–969.

Carey, L. D., and S. A. Rutledge (2000), The relationship between precipitation and lightning in tropical island convection: A C-band polarimetric radar study, Mon. Wea. Rev., 128, 2687–2710.

Cummins, K. L., and M. J. Murphy (2009), An overview of lightning locating systems: History, techniques, and data uses, with an in-depth look at the U. S. NLDN, IEEE Trans. Electromagn. Compat., 51, 499–518.

Dye, J. E., W. P. Winn, J. J. Jones, and D. W. Breed (1989), The electrification of New Mexico thunderstorms. Part 1: Relationship between precipitation development and the onset of electrification, J. Geophys. Res., 94, 8643–8656.

El-Magd, A., V. Chandrasekar, V. N. Bringi, and W. Strapp (2000), Multiparameter radar and *in situ* aircraft observation of graupel and hail, IEEE Trans. Geosci. Rem. Sens., 38, 570–578.

Germann, U., and I. Zawadzki (2002), Scale-dependence of the predictability of precipitation from continental radar images. Part I: Description of the methodology, Mon. Wea. Rev., 130, 2859–2873.

Gremillion M. S., and R. E. Orville (1999), Thunderstorm characteristics of cloud−to−ground lightning at the Kennedy Space Center, Florida: A study of lightning initiation signatures as indicated by WSR−88D, Wea. Forecasting, 14, 640−649.

Lim, S., V. Chandrasekar, and V. N. Bringi (2005), Hydrometeor classification system using dual-polarization radar measurements: Model improvements and *in situ* verification, IEEE Trans. Geosci. Rem. Sens., 43, 792–801.

Milbrandt, J. A. and M. K. Yau (2005), A multimoment bulk microphysics parameterization. Part II: A proposed three-moment closure and scheme description, J. Atmos. Sci., 62, 3065–3081.

Mosier, R. M., C. Schumacher, R. E. Orville, and L. D. Carey (2011), Radar nowcasting of cloud-to-ground lightning over Houston, Texas, Wea. Forecasting, 26, 199–212.

Orville, R. E. (2008), Development of the National Lightning Detection Network, Bull. Amer. Meteor. Soc., 89, 180–190.

Pearson K. (1896), Mathematical contributions to the theory of evolution. III. Regression, heredity, and panmixia. Phil. Trans. Roy. Soc. Ser. A, 187, 253–318.

Petersen, W. A. (1997), Multi-scale process studies in the tropics: Results from lightning observations, Ph.D. dissertation, 354 pp., Colorado State University, 21 March.

Ruzanski, E. , V. Chandrasekar, and Y. Wang (2011), The CASA nowcasting system, J. Atmos. Oceanic Technol., 28, 640–655.

Ruzanski, E., and V. Chandrasekar (2012), An investigation of the short-term predictability of precipitation using high-resolution composite radar observations, J. Appl. Meteor. Climatol., 51, 912–925.

Seroka, G. N., R. E. Orville, and C. Schumacher (2012), Radar nowcasting of total lightning over the Kennedy Space Center, Wea. Forecasting, 27, 189–204.

Vamoș, C., and M. Crăciun, (2012), Automatic Trend Estimation. Springer, The Netherlands.

Vincent, B. R, L. D. Carey, D. Schneider, K. Keeter and R. Gonski (2003), Using WSR-88D reflectivity data for the prediction of cloud-to-ground lightning: A North Carolina study, Nat. Wea. Digest, 27, 35–44.

Wolf, P. (2006), Anticipating the initiation, cessation, and frequency of cloud-to-ground lightning, utilizing WSR-88D reflectivity data, NWA Elec. J. Operational Meteor, December 2006.

Wainwright, C. E., D. T. Dawson II, M. Xue, and G. Zhang (2014), Diagnosing the intercept parameters of the exponential drop size distributions in a single-moment microphysics scheme and impact on supercell storm simulations, J. Appl. Meteor. Climatol., 53, 2072–2090.

Woodard, C. J., L. D. Carey, W. A. Petersen, and W. P. Roeder (2012), Operational utility of dual-polarization variables in lightning initiation forecasting, Elec. J. Operational Meteor., 13, 79–102.

Yang, Y. H., P. King (2010), Investigating the potential of using radar echo reflectivity to nowcast cloud-to-ground lightning initiation over Southern Ontario, Wea. Forecasting, 25, 1235–1248.

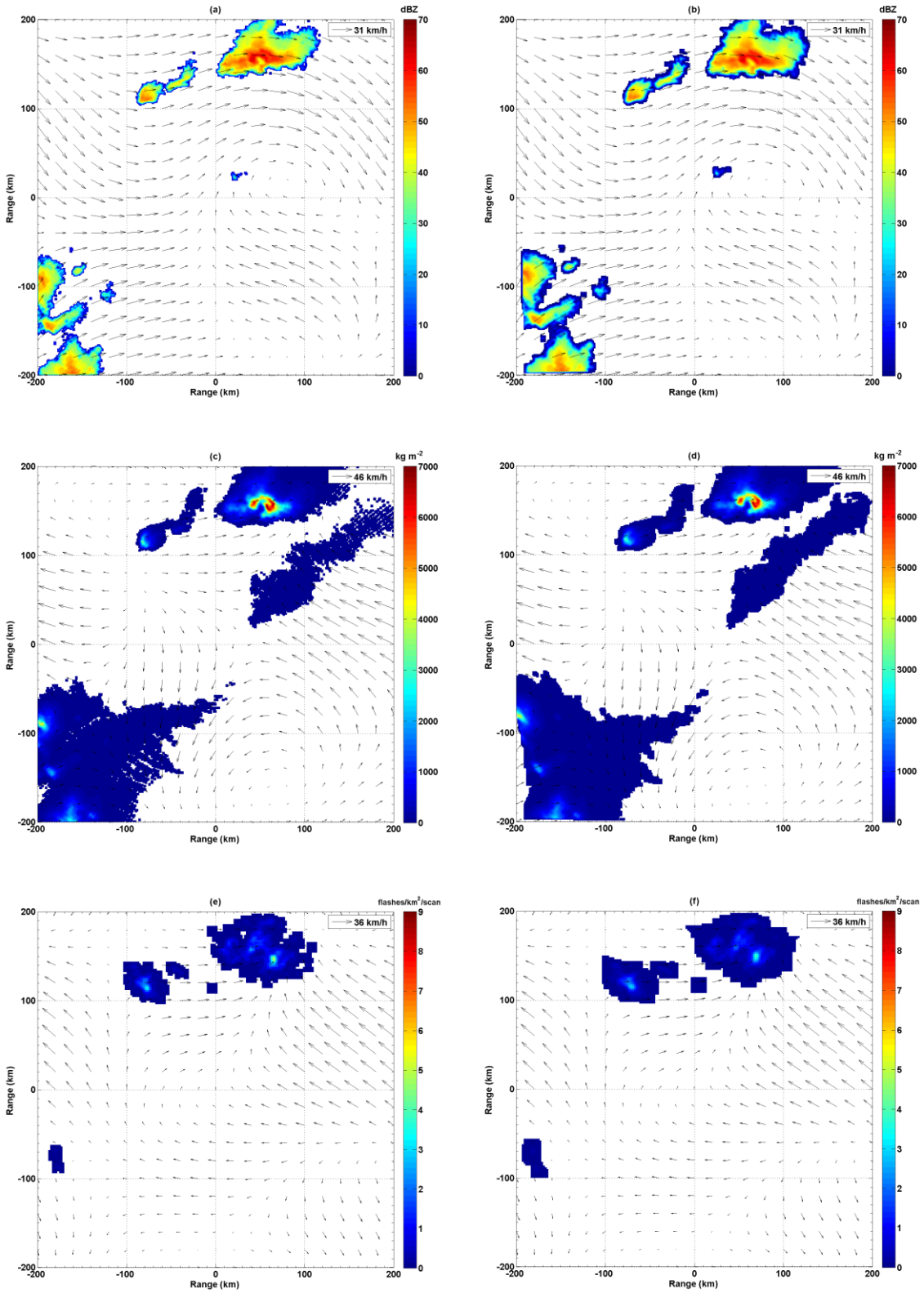

Fig. 1. (a) Reflectivity, (c) Vertically Integrated Ice, and (e) lightning density observations with DARTS-estimated motion vector fields for 2320 UTC 03 Apr 2014. Corresponding nowcasts valid at 2334 UTC 03 Apr 2014 are shown in panels (b), (d), and (f), respectively.

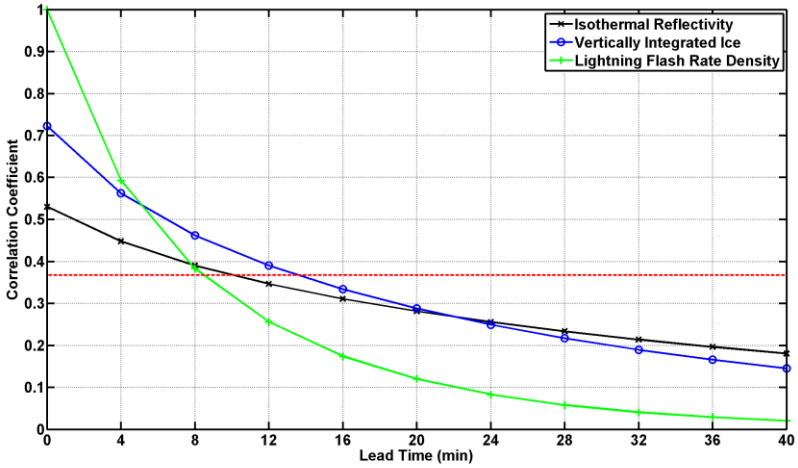

Fig. 2. Cross-correlation coefficients between nowcasts of isothermal reflectivity (ZH), Vertically Integrated Ice (VII), and lightning density (LGT) and the time-aligned lightning observations vs. nowcast lead time. The cross-correlation coefficient values shown represent the average over the four events studied. The dashed horizontal line corresponds to a cross-correlation coefficient value of 1/*e* showing an estimate of the de-cross-correlation times (i.e., predictability) for each product.